L-2L De-embedding Method with Double-T-type PAD Model for Millimeter-wave Amplifier Design

Seitaro Kawai, Korkut Kaan Tokgoz, Kenichi Okada, and Akira Matsuzawa

Dept. Physical Electronics, Tokyo Institute of Technology
2-12-1-S3-27, Ookayama, Meguro-ku, Tokyo 152-8552 Japan.
Tel: +81-3-5734-3764, Fax: +81-3-5734-3764
E-mail: kawai@ssc.pe.titech.ac.jp

***Abstract*— For millimeter-wave CMOS circuit design, accurate device models are necessary. Especially an accurate de-embedding method is very important. Hence, precise de-embedding of pad parasitics is the first and valuable step to achieve accurate device models. In this work, a new pad modeling based on an L-2L de-embedding is proposed. The pad model is derived with an assumption that characteristic impedance of transmission line becomes constant at high frequency. Every device used in an amplifier is characterized with the proposed de-embedding method, and simulation and measurement results well agree with each other up to 110 GHz.**

***Index Terms*— De-embedding, mm-Wave, modeling, transmission line, CMOS**

I. Introduction

Wireless communication systems in millimeter-wave (mm-wave) frequency range attracts attention from both industry and academia in order to achieve high data-rate systems. One of the best candidate mm-wave frequency range to achieve several Gbps data-rate is 60 GHz carrier, where an unlicensed 9 GHz bandwidth can be used. This 9 GHz unlicensed band enables tens of Gbps communication with a proper modulation scheme [1], [2]. For a complete TRX to be implemented with desired performances, accurate active and passive device characterization and modeling is needed, because the models provided by foundries, unfortunately, are not accurate at mm-wave frequency. Moreover, several customized devices are essential. The very first part of device characterization is the de-embedding process, which is used to remove the effects of test fixtures (probing pads' characteristics) from measured results of any kind of Test Element Group (TEG).

There are vast number of studies about de-embedding. In [3], several de-embedding methods ([4]-[6]) are discussed on the characterization and modeling of transmission lines (TLs) and their influence on amplifier response. According to [3], L-2L method is the most accurate method [6]. Still, L-2L method is not accurate enough in very high frequencies. The reason of this inaccuracy is the available less information from the measurements then required, since in all of the mentioned methods there are two results which can be solved for two unknowns. Actually, the pad responses are not symmetrical but reciprocal. As a result, the pads should be characterized with three variables for more accurate de-embedding.

Referring to these reasons, in this paper, a new pad model is constructed with three components, and the calculation method to solve three parameters are presented with the results of L-2L de-embedding method and using the assumption of constant characteristic impedance of TLs at high frequencies.

II. Conventional Pad Model

To use L-2L method, two TLs are needed, the length of one is twice the length of the other. Fig. 1 briefly illustrates the L-2L de-embedding method.

In terms of T-parameters it is expressed as follows;

$$\boldsymbol{T}_{\mathrm{meas}} = \boldsymbol{T}_{\mathrm{Lpad}}\boldsymbol{T}_{\mathrm{DUT}}\boldsymbol{T}_{\mathrm{Rpad}} \quad (1)$$

$$\boldsymbol{T}_{\mathrm{L+pad}} = \boldsymbol{T}_{\mathrm{Lpad}}\boldsymbol{T}_{\mathrm{L}}\boldsymbol{T}_{\mathrm{Rpad}} \quad (2)$$

$$\boldsymbol{T}_{\mathrm{2L+pad}} = \boldsymbol{T}_{\mathrm{Lpad}}\boldsymbol{T}_{\mathrm{2L}}\boldsymbol{T}_{\mathrm{Rpad}} \ (\boldsymbol{T}_{2L} = \boldsymbol{T}_{L}\boldsymbol{T}_{L}) \quad (3)$$

$$\boldsymbol{T}_{\mathrm{thru}} = \boldsymbol{T}_{\mathrm{Lpad}}\boldsymbol{T}_{\mathrm{Rpad}} = \boldsymbol{T}_{\mathrm{L+pad}}\boldsymbol{T}_{\mathrm{2L+pad}}^{-1}\boldsymbol{T}_{\mathrm{L+pad}} \quad (4)$$

Here, $\boldsymbol{T}_{\mathrm{L+PAD}}$ and $\boldsymbol{T}_{\mathrm{2L+PAD}}$ are the measurement results of TLs. $\boldsymbol{T}_{\mathrm{LPAD}}$ and $\boldsymbol{T}_{\mathrm{RPAD}}$ are the T-parameters of left pad and right pad, respectively.

Since the measurement results of TL TEGs are symmetric and reciprocal, the thru has two known values in terms of S-, Y-, or Z-parameter. On the other hand, because pads are reciprocal passive device, they are supposed to be expressed by at least three parameters (double-T-type) pad model using three parameters shown in Fig. 2. It is impossible to determine these three parameters (Z_1, Z_2, Z_3) due to the limitations of the calculation of L-2L method, some approximation is required. Thus, only using the thru response the pads can be modeled as

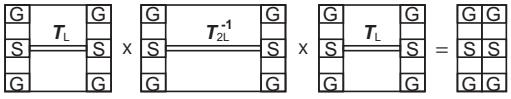

Fig. 1. Graphical illustration of L-2L de-embedding method.

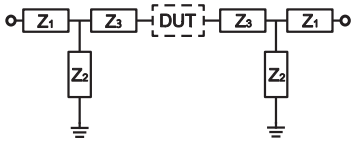

Fig. 2. Proposed double-T-type pad model.

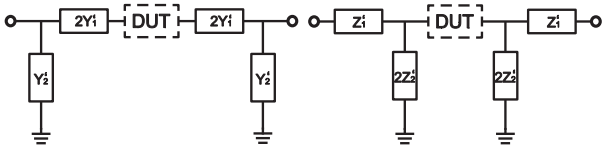

(a) π-type pad model. (b) T-type pad model.

Fig. 3. Conventional pad models.

the combination of one shunt admittance and one series impedance with two different versions as π-type (Fig. 3(a)) and T-type (Fig. 3(b)) circuits. Left-pad and right-pad can be expressed by Y-parameters using π-type as follows;

$$\boldsymbol{Y}_{\text{thru}\_\pi} = \begin{bmatrix} Y_{11} & Y_{12} \\ Y_{21} & Y_{22} \end{bmatrix} = \begin{bmatrix} Y_1^{'} + Y_2^{'} & -Y_1^{'} \\ -Y_1^{'} & Y_1^{'} + Y_2^{'} \end{bmatrix} \tag{5}$$

$$\boldsymbol{Y}_{\text{Lpad}\_\pi} = \begin{bmatrix} Y_{11} - Y_{12} & 2Y_{12} \\ 2Y_{12} & -2Y_{12} \end{bmatrix} \boldsymbol{Y}_{\text{Rpad}\_\pi} = \begin{bmatrix} -2Y_{12} & 2Y_{12} \\ 2Y_{12} & Y_{11} - Y_{12} \end{bmatrix}$$

Similarly, T-type of thru is given in terms of Z-parameters in Eq. (6). Again in a similar way, Z-parameters of left-pad and right-pad are provided.

$$\boldsymbol{Z}_{\text{thru\_T}} = \begin{bmatrix} Z_{11} & Z_{12} \\ Z_{21} & Z_{22} \end{bmatrix} = \begin{bmatrix} Z_1^{'} + Z_2^{'} & Z_2^{'} \\ Z_2^{'} & Z_1^{'} + Z_2^{'} \end{bmatrix} \tag{6}$$

$$\boldsymbol{Z}_{\text{Lpad\_T}} = \begin{bmatrix} Z_{11} + Z_{12} & 2Z_{12} \\ 2Z_{12} & 2Z_{12} \end{bmatrix} \boldsymbol{Z}_{\text{Rpad\_T}} = \begin{bmatrix} 2Z_{12} & 2Z_{12} \\ 2Z_{12} & Z_{11} + Z_{12} \end{bmatrix}$$

TLs is expressed as follows in terms of F-parameter (ABCD-parameter);

$$\boldsymbol{F}_{\text{TL}} = \begin{bmatrix} \cos\gamma\ell & Z_0 \sin\gamma\ell \\ \frac{1}{Z_0}\sin\gamma\ell & \cos\gamma\ell \end{bmatrix} \tag{7}$$

When double-T-type pad model is de-embedded by the π-type and T-type pad model, the de-embedded results can be expressed as following equation in terms of F-parameter.

$$\boldsymbol{F}_{\text{TL}\_\pi} = \boldsymbol{F}_{\text{Lpad}\_\pi}^{-1} \boldsymbol{F}_{\text{Lpad}} \boldsymbol{F}_{\text{TL}} \boldsymbol{F}_{\text{Rpad}} \boldsymbol{F}_{\text{Rpad}\_\pi}^{-1} \tag{8}$$

$$= \begin{bmatrix} \cos\gamma\ell & Z_0 (\frac{Z_1}{Z_2} + 1)^2 \sin\gamma\ell \\ \frac{1}{Z_0 (\frac{Z_1}{Z_2} + 1)^2} \sin\gamma\ell & \cos\gamma\ell \end{bmatrix} \tag{9}$$

$$\boldsymbol{F}_{\text{TL\_T}} = \boldsymbol{F}_{\text{Lpad\_T}}^{-1} \boldsymbol{F}_{\text{Lpad}} \boldsymbol{F}_{\text{TL}} \boldsymbol{F}_{\text{Rpad}} \boldsymbol{F}_{\text{Rpad\_T}}^{-1} \tag{10}$$

$$= \begin{bmatrix} \cos\gamma\ell & \frac{Z_0}{(\frac{Z_3}{Z_2} + 1)^2} \sin\gamma\ell \\ \frac{(\frac{Z_3}{Z_2} + 1)^2}{Z_0} \sin\gamma\ell & \cos\gamma\ell \end{bmatrix} \tag{11}$$

Here, $\boldsymbol{F}_{\text{L,Rpad}\_\pi,\text{T}}$ are the left or right pad model of π or T -model. $\boldsymbol{F}_{\text{L,Rpad}}$ are the left and right pad model of double-T-model shown in Fig. 2.

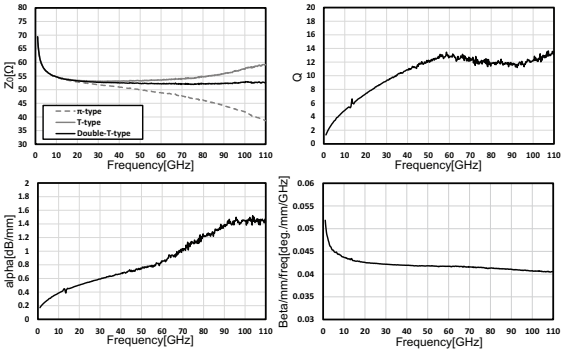

Fig. 4. Comparison of TL characteristics.

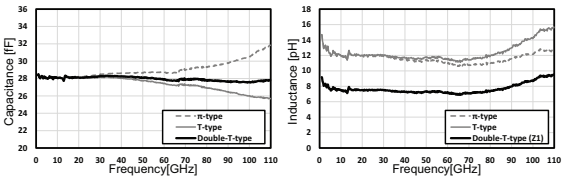

Fig. 5. Comparison of pad models.

Thus, Q, α, and β characteristics of TLs are not different depending on the pad model but the characteristic impedance is different. When de-embedded by π-type, a $(\frac{Z_1}{Z_2} + 1)^2$ fold difference occurs only in the characteristic impedance. Also a $1/(\frac{Z_3}{Z_2} + 1)^2$ fold difference occurs only in the characteristic impedance by T-type pad model.

Fig. 4 compares the characteristics of the de-embedded TLs for π-type and T-type circuit of pads. It can be observed that Q, α, and β characteristics of TLs are same with each other for the two cases, but the difference between the two cases on characteristic impedance is getting larger after 20 GHz. However, it is well-known from the theory that the characteristic impedance of TL should be constant when the frequency is high, and this relation is given by the following equation;

$$Z_0 = \sqrt{\frac{R + j\omega L}{G + j\omega C}} \cong \sqrt{\frac{L}{C}} (\omega L \gg R, \omega C \gg G) \tag{12}$$

The reason of this difference can be understood by observing Fig. 5, which shows the capacitance and inductance of π- and T-type circuit of pads, accordingly. The characteristic impedance behavior and capacitance of the pad models have a direct relation. The π-model over estimates the capacitance and characteristic impedance gets smaller as the frequency increases. The counterpart of this comment can be said for T-type-model. Moreover, the capacitance of the pad resulted between top-metal and ground can be assumed constant.

III. Proposed Pad Model

As discussed in the previous section π-type or T-type pad models are expressed by two parameters ($Y_1^{'}$,$Y_2^{'}$ or $Z_1^{'}$,$Z_2^{'}$) due to limitations of the calculation of L-2L method. However, three parameters should be needed to realize the

reciprocal passive components modeling. As mentioned, because only two parameters can be obtained from the L-2L calculation, it is necessary to put some assumption. Here, following equation is assumed:

$$Z_3 = \mathrm{k} \times Z_1 \ (0 \leq k \leq 1) \tag{13}$$

From this assumption, Z_1 and Z_2 can be expressed as follow by using conventional T-type results.

$$Z_1 = Z_1^{'} + \frac{Z_2^{'}}{2}(k+1-\sqrt{k^2+2k+1+4k\frac{Z_1^{'}}{Z_2^{'}}}) \tag{14}$$

$$Z_2 = \frac{2k(Z_1^{'}+Z_2^{'})}{k-1+\sqrt{k^2+2k+1+4k\frac{Z_1^{'}}{Z_2^{'}}}} \tag{15}$$

Then, "k" is adjusted such that the capacitor remains relatively constant up to 110 GHz. This time, k is found to be 0.4. Better to note that this value might change with different processes and different structures of pads and TLs. Fig. 5 shows the capacitance and the inductance values of the calculated proposed pad model in comparison with π-, and T-type. In the inductance of proposed pad mode, only Z_1 is included, that of Z_3 is not included. One can observe that the capacitance of the proposed pad model remains almost constant up to 110 GHz. Moreover, Fig. 4 provides Z_0, Q, α and β of characteristics of de-embedded TL by the proposed pad model. Compared to the results in Fig. 4, Q, α and β are same and the characteristic impedance become constant in the high frequency regime. One can conclude that the proposed de-embedding is more accurate than the conventional methods.

IV. Evaluation with 1-stage Amplifier Results

To evaluate the accuracy of de-embedding, a 1-stage amplifier is designed, manufactured and measured. Fig. 6(a) provides the schematic of the amplifier and Fig. 6(b) shows the micro-graph of amplifier. This amplifier is constructed with TLs, bend lines, transistor (gate length of 60 nm and gate width of 2 µm by 20 fingers), MOM-capacitor (150 fF), and decoupling transmission line (Metal-Insulator-Metal Transmission Line (MIM TL)). These components are characterized after de-embedding of proposed pad model. The comparison of the measurement and modeled results of S_{21}, S_{11} and S_{22} is given in Fig. 7. S_{21} and S_{11} of the simulation results have good agreement with the measurement result. However, S_{22} of the simulation result is a bit different from the measurement result, which is caused by MIM TL modeling error. Because of the low impedance of MIM TL ($2\,\Omega \sim 3\,\Omega$), it is difficult to obtain accurate measurement results in a 50 Ω system.

V. Conclusion

Accuracy of conventional de-embedding methods are discussed, and it is concluded that symmetrical and reciprocal pad characteristics are not accurate enough in the

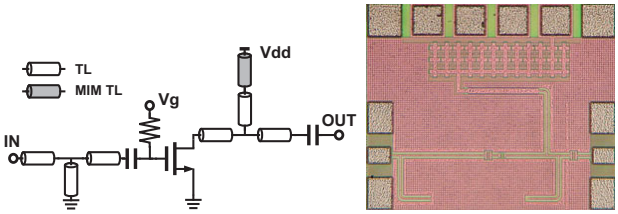

(a) schematic. (b) die photo.

Fig. 6. 1-stage amplifier.

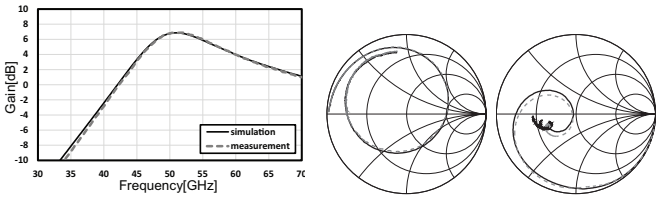

(a) S_{21}. (b) S_{11}. (c) S_{22}.

Fig. 7. The comparison of modeled and measured amplifier.

mm-wave range. Hence, a three element -just reciprocal- pad model is proposed along with its calculation method. The characteristic impedance of the de-embedded TLs with the proposed method remains constant in high frequencies as the theory states. Furthermore, with the new de-embedding method, several devices are characterized and its validity is evaluated with the measurement results of a 1-stage amplifier. The comparison in amplifier characteristics demonstrates accuracy of the proposed method.

Acknowledgment

This work is partially supported by MIC, SCOPE, MEXT, STARC, STAR and VDEC in collaboration with Cadence Design Systems, Inc., Mentor Graphics, Inc., and Agilent Technologies Japan, Ltd.

References

[1] K. Okada, *et al.*, "A full 4-Channel 6.3 Gb/s 60 GHz direct-conversion transceiver with low-power analog and digital baseband circuitry," in *IEEE ISSCC Digest of Technical Papers*, pp. 218-219, Feb. 2012.

[2] V. Vidojkovic, *et al.*, "A low-power radio chipset in 40nm LP CMOS with beamforming for 60 GHz high-data-rate wireless communication," in *IEEE ISSCC Digest of Technical Papers*, pp. 236-237, Feb. 2013.

[3] R. Minami, C. Han, K. Matsushita, K. Okada, and A. Matsuzawa, "Effect of transmission line modeling using different de-embedding methods," in *EuMC*, pp. 381-384, Dec. 2011.

[4] M. Koolen, J. Geelen, and M. Versleijen, "An improved de-embedding technique for on-wafer high-frequency characterization," in *Proc. Bipolar/BiCMOS Circuits and Tech. Meeting*, Sep. 1991, pp. 188-191.

[5] H. Ito, K. Masu, "A simple through only de embedding method for on wafer s parameter measurements up to 110 GHz," in *IEEE MTT-S*, Jun 2008, pp. 383-386.

[6] J. Song, F. Ling, G. Flynn, W. Blood, and E. Demircan, "A de-embedding technique for interconnects," in *Electrical Performance of Electronic Packaging*, Oct. 2001, pp. 129-132.

[7] T. Sekiguchi, S. Amakawa, N. Ishihara, and K. Masu, "On the validity of bisection-based thru-only de-embedding," in *IEEE International Conference on Microelectronic Test Structures*, pp. 66-71, Mar. 2010.